

Analytical Approaches for Fast Computing of the Thermal Load of Vehicle Cables of Arbitrary Length for the Application in Intelligent Fuses

Anika Henke^a and Stephan Frei^b

On-board Systems Lab, TU Dortmund University, Otto-Hahn-Str. 4, Dortmund, Germany

Keywords: Analytical Approaches, Axial Heat Transfer, Green's Functions, Intelligent Electronic Fuses, Laplace Transform, Smart Fuses, Thermal Cable Model, Transient Temperature Computation, Vehicle Cable Systems.

Abstract: In modern intelligent vehicles, a huge number of components leads to complex cable harnesses with high reliability demands. Static connections protected by simple melting fuses are more and more replaced by intelligent power distribution and switching units. Thermal considerations play an important role with respect to reliability as thermal overload situations can lead to accelerated aging, damaged cables and finally to interruptions in the power supply. The calculation of the axial transient temperature distribution in cable structures is a complex task that is often solved numerically. In this paper, two analytical approaches to model the temperature of a single cable in air are presented, that are based on the use of Green's functions in the time domain respectively Laplace domain. As sums appear, the convergence behavior is evaluated. The approaches are validated using a numerical reference solution. The influence of the cable length on the accuracy of the solutions is examined and complexity considerations are performed. An application example for intelligent vehicles is presented and discussed.

1 INTRODUCTION

The development of intelligent and connected vehicles is an ongoing process reaching for improved safety, efficiency and user comfort. In addition to established basic functions, a huge variety of features for automated driving is added. All those features require highly reliable power supply systems (Kong et al., 2019) depending on their safety relevance: Failure in entertainment systems is disturbing but not critical, whereas failure in safety-critical systems (e.g. autonomous driving functions) is crucial and must not appear.

Classically, the electrical power supply is statically connected to the loads. The connecting cables are protected with simple melting fuses as shown in Figure 1(a). During the cable harness development, those cables and fuses must be dimensioned considering the maximum expected currents to avoid overload under all operating states. Based on an estimated worst-case current pulse, that

might appear extremely seldom, an appropriate cable needs to be chosen. Therefore, cables can be over-dimensioned for the regular operating states (Horn et al., 2018). Once under operation, the highly temperature depending aging process in the cable begins. Using melting fuses, the duration of a maximum load condition and the real cable temperature cannot be monitored, so the remaining lifetime cannot be estimated.

In recent vehicle developments, intelligent power distribution units (PDUs) with integrated intelligent fuses become more widespread (Kong et al., 2019) as shown in Figure 1(b). Such a PDU can flexibly switch

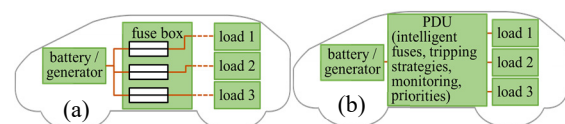


Figure 1: Power supply in a vehicle (a) a static connection with melting fuses or (b) a PDU for flexible and intelligent switching options.

^a <https://orcid.org/0000-0001-5028-4767>

^b <https://orcid.org/0000-0002-8917-3914>

loads on and off for functional but also fusing purposes. It is possible to control the power flow according to safety demands. Thus, highly safety-critical systems can be prioritized regarding their power demands. The actual cable insulation temperature and aging status can be monitored based on the load history to evaluate the safety of operation at any time. This enables the operation closer to the cable limits, i.e. smaller cross sections can be chosen or temporarily the current can be increased. Therefore, more options are available in the decision process and different strategies can be implemented depending on the safety relevance of the connected systems. For example, a simple on/off switching strategy can be used that interrupts the current if a predefined temperature limit is exceeded and switches it on again as soon as the temperature falls below a second defined temperature as e.g. mentioned in (Önal et al., 2020). So, the usage of an intelligent fuse can enhance the availability and reliability of the complete system or reduce its weight as over-dimensioned cables can be avoided. To enable a reasonable switching decision, the cable insulation temperature has to be known.

As the insulation temperature often cannot be measured directly, thermal cable models based on current measurements are necessary. If additional information (e.g. the environmental temperature) is available, it can also be considered. Otherwise, worst-case assumptions are necessary.

Thermal cable models to be integrated into PDUs with cheap and less powerful microcontrollers should be as simple as possible. Very basic analytical models that neglect the axial heat flow along the cable (e.g. (Zhan et al., 2019) or (Olsen et al., 2013)) or the transient temperature development (e.g. (Brabetz et al., 2011) or (Holyk et al., 2014)) cannot predict the cable temperature very precisely. More complex models are often based on a two- or three-dimensional model of the cable which is used for the numerically based simulation of the cable temperatures as, e.g., in (He et al., 2013). Nearly arbitrary environmental and load conditions can be modelled this way, but these methods require high computational effort. This effort can be drastically reduced by using analytical methods. In this paper, two different methods for analytical temperature calculations using Green's functions are presented and discussed. Those allow a precise temperature calculation with low effort for a single insulated cable under special conditions based on the known current.

In chapter 2, the fundamental model is presented. Earlier research is shortly summarized. The new analytical solution methods based on the use of

Green's functions in the time domain respectively Laplace domain are introduced in chapter 3. In chapter 4, those new methods are validated and compared to earlier developed methods with regard to their performance. In chapter 5, an application example is discussed: Failure leads to an overcurrent that causes a melting fuse to trip. Unlike, with an intelligent fusing strategy, the overload can be tolerated, and important automated driving applications can still be provided. An uncontrolled system breakdown is avoided.

2 PRELIMINARY WORK

This section is based on (Henke and Frei, 2020). There, the fundamental model was presented for a single cable of length L oriented in z -direction consisting of a conductor (radius r_c) and an insulation (outer radius r_i) as shown in Figure 2(a). A current I flows through the cable. The equivalent circuit for an infinitesimally short cable segment shown in Figure 2(b) is used. Per unit length (pul) quantities are marked with an upstroke. The pul heat source P'_e represents the cable heating induced by the current I that flows through the conductor and depends on the conductor temperature T . The pul capacitance C' is used to model the heat storing capacity of the complete cable (conductor and insulation). The pul admittance G' describes the heat conduction through the insulation layer and the heat transfer from the cable to the ambient air via convection and radiation and depends on the cable surface temperature T_s and the ambient air temperature T_e . The axial heat flow in the conductor is modelled using the pul resistance R' . The axial heat flow in the insulation is neglected due to the low thermal conductivity of the insulation compared to the conductor.

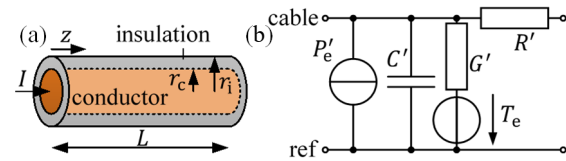


Figure 2: (a) Examined single cable. (b) Thermoelectric equivalent circuit for infinitesimally short cable segment.

From this equivalent circuit, the partial differential equation (1) is derived for the conductor temperature $T(z, t)$ with the initial and boundary conditions (2).

$$\partial^2 T / \partial z^2 - A \partial T / \partial t - B T = -C, \quad (1)$$

$$A = R' C', B = R' G', C = R' (G' T_e - P'_e), \\ T(z, 0) = T_0, T(0, t) = T_1, T(L, t) = T_2. \quad (2)$$

This differential equation can be solved using the Laplace transform. In the Laplace domain, an ordinary differential equation remains, and an analytical solution is found. Using the approximation (3), which is valid for long cables (large L), the analytical expression (4) in the time domain is calculated.

$$e^{-L\sqrt{R'(G'+C's)} \pm 1} \approx \pm 1, \tag{3}$$

$$D_1(z) = \operatorname{erf}\left(z\sqrt{A/(4t)}\right) \tag{4}$$

$$D_2(z) = e^{-|z|\sqrt{B}} \left\{ \operatorname{erf}\left(\frac{A|z| - 2\sqrt{B}t}{2\sqrt{At}}\right) - 1 \right\} + e^{|z|\sqrt{B}} \left\{ \operatorname{erf}\left(\frac{A|z| + 2\sqrt{B}t}{2\sqrt{At}}\right) - 1 \right\}, z_L = L - z,$$

$$T_L(z, t) = \frac{C}{B} + \left(\frac{C}{B} - T_0\right) e^{-\frac{B}{A}t} [1 - D_1(z_L) - D_1(z)] + \left(\frac{C}{B} - T_1\right) \frac{D_2(z)}{2} + \left(\frac{C}{B} - T_2\right) \frac{D_2(z_L)}{2}.$$

As already mentioned above, the parameters P'_e and G' in the equivalent circuit are not constant but depend on the cable and surface temperatures. This nonlinear dependency was neglected in the above presented solution. To take it into account, an iterative solution approach was developed in (Henke and Frei, 2020) and is shortly resumed here: After an initialization, the surface temperature T_s and the parameters P'_e and G' are calculated. Those are used to find the conductor temperature T . As termination condition, the absolute difference $\sigma_T = |T^k - T^{k+1}|$ between two iterations is calculated. The process is continued until this difference falls below $\Delta_{T,Limit} = 0.001$ K. In Figure 3, this approach is summed up.

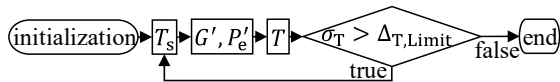


Figure 3: Iterative approach for nonlinearities.

3 APPROACHES BASED ON GREEN'S FUNTIONS

In this section, two new approaches for the solution of the partial differential equation (1) are presented. Both of them are based on Green's functions.

3.1 Time Domain Approach

In this approach, Green's functions are used to solve the partial differential equation directly in the time domain. The problem can be classified as

inhomogenous differential equation with inhomogenous boundary and initial conditions as generally, C, T_0, T_1 and T_2 are not zero. According to the principle of superposition, the complete solution results as superposition of solutions that take into account only one of the inhomogeneities assuming the others to vanish:

$$T_G(z, t) = T_G|_{C=T_1=T_2=0} + T_G|_{T_0=T_1=T_2=0} + T_G|_{C=T_0=T_2=0} + T_G|_{C=T_0=T_1=0} \tag{5}$$

From the corresponding Green's function (6), the different solution parts (eq. (7)) are calculated. The solution for $T_2 \neq 0$ is calculated using the solution for $T_1 \neq 0$ by replacing T_1 with T_2 and z with $L - z$ due to symmetry considerations. The superposition of all four parts leads to the complete solution (8).

$$L_n = 2nL, G_{X11}(z, t|z_0, \tau) = \frac{e^{-\frac{B}{A}t}\sqrt{-A}}{2\sqrt{\pi(t-\tau)}} \tag{6}$$

$$\cdot \sum_{n=-\infty}^{\infty} \left[e^{\frac{A(L_n+z-z_0)^2}{4(t-\tau)}} - e^{\frac{A(L_n+z+z_0)^2}{4(t-\tau)}} \right],$$

$$T_G|_{C=T_1=T_2=0} = \int_0^L G_{X11}(z, t|z_0, 0) T_0 dz_0, \tag{7}$$

$$T_G|_{T_0=T_1=T_2=0} = \int_0^t \int_0^L G_{X11}(z, s|z_0, 0) C dz_0 ds,$$

$$\Psi(z, t) = \sqrt{-1/(A\pi t)} \partial_z \sum_{n=-\infty}^{\infty} e^{\frac{A(L_n+z)^2}{4t} - \frac{B}{A}t},$$

$$T_G|_{C=T_0=T_2=0} = \int_0^t \Psi(z, s) T_1 ds.$$

$$T_G(z, t) = T_L(z, t) \tag{8}$$

$$+ \sum_{n=1}^{\infty} (C/B - T_0) e^{-Bt/A} [D_1(-z_L + L_n) + D_1(-z_L - L_n) - D_1(z + L_n) - D_1(z - L_n)] + 0.5[(C/B - T_1)\{D_2(z + L_n) - D_2(z - L_n)\} + (C/B - T_2)\{D_2(z_L + L_n) - D_2(z_L - L_n)\}].$$

Here, the earlier term from the solution in the Laplace domain $T_L(z, t)$ appears again and is extended by additional terms. This new solution is complete, as no approximations were necessary. Nevertheless, because of the infinite sum, in an implementation only a finite number of terms can be considered, which results in an approximation.

3.2 Laplace Domain Approach

The second new approach operates in the Laplace domain as the earlier described solution. There, some terms caused problems with the transform back into the time domain as expressions with several exponential functions depending on \sqrt{s} needed to be

transformed. To avoid this problem, using Green's functions, expressions are derived, that can be transformed back into the time domain more easily. This approach is used in the electrical transmission line theory as well (Antonini, 2008). For homogenous boundary conditions (9) the conductor temperature T_{GL} is calculated via eq. (10) from the Laplace domain Green's function G_T of the problem (11).

$$0 = T_{GL}(z, s)|_{z=0} = T_{GL}(z, s)|_{z=L}, \quad (9)$$

$$T_{GL}(z, s) = - \int_0^L G_T(z, z_0, s) I_s dz_0, \quad (10)$$

$$I_s = AT_0 + C/s.$$

$$G_T(z, z_0, s) = - \frac{2}{L} \sum_{n=1}^{\infty} \frac{\psi_n(z)\psi_n(z_0)}{(sA + B) + n_L^2}, \quad (11)$$

$$\psi_n(z) = \sin(n_L z), n_L = n\pi/L.$$

A series approach for the Green's function is used instead of the direct usage of the Green's function of the Helmholtz equation. This way, the result in the Laplace domain (12) can easily be transformed back into the time domain (see eq. (13)).

$$T_{GL}(z, s) = \frac{4I_s}{L} \sum_{m=0}^{\infty} \frac{\sin(m_L z)}{(sA + B) + m_L^2} \frac{1}{m_L}, \quad (12)$$

$$T_{GL}(z, t) = 4/L \cdot \sum_{m=0}^{\infty} \frac{\sin(m_L z)/m_L}{\left[T_0 e^{-\frac{t}{A}[m_L^2+B]} + C \left(1 - e^{-\frac{t}{A}[m_L^2+B]} \right) / (B + m_L^2) \right]}. \quad (13)$$

By now, homogenous boundary conditions were assumed. The result can be applied for inhomogenous boundary conditions (14) by setting the reference temperature to $T_1 = T_2$. If the cable end temperatures are not equal, the expansion (15) is necessary. The transformation back into the time domain leads to eq. (16). The boundary conditions at $z = 0$ m and $z = L$ are fulfilled for the limit (17), but this solution is unsteady at the cable ends.

$$\begin{aligned} T_{GL}(z, t)|_{z=0} &= T_1 \\ &= T_{GL}(z, t)|_{z=L} = T_2 \neq 0 \end{aligned} \quad (14)$$

$$T_{GL,i}(z, s) = \frac{T_2}{s} \frac{d}{dz_0} G_T(z, z_0, s)|_{z_0=L} \quad (15)$$

$$- T_1/s \frac{d}{dz_0} G_T(z, z_0, s)|_{z_0=0} + T_{GL}(z, s)$$

$$T_{GL,i}(z, t) = T_{GL}(z, t) \quad (16)$$

$$+ \frac{2}{\pi} \sum_{n=1}^{\infty} \left[1 - e^{-\frac{n_L^2-B}{A}t} \right] \frac{n_L^2 \sin(n_L z)}{n(n_L^2 - B)} [T_1 - (-1)^n T_2]$$

$$\lim_{z \rightarrow 0} T_{GL,i}(z, t) = T_1, \lim_{z \rightarrow L} T_{GL,i}(z, t) = T_2. \quad (17)$$

Additionally, the expansion converges slowly (see section 4.3). So, the practical applicability is limited.

4 VALIDATION

In this section, the derived approaches are evaluated. If not stated differently, the following 6 mm²-cable is evaluated: The solid copper conductor has the radius $r_c = 1.382$ mm, the specific heat capacity $c_c = 3.4 \cdot 10^6$ J/m³K, the thermal conductivity $\lambda_c = 386$ W/Km and the resistivity $\rho = 1.86 \cdot 10^{-8}$ Ω m at 20 °C. The linear temperature coefficient is $\alpha_T = 3.93 \cdot 10^{-3}$ 1/K. The conductor is surrounded by a PVC insulation. The total radius of the cable with insulation is $r_i = 2$ mm. The specific heat capacity of the insulation material is $c_i = 2.245 \cdot 10^6$ J/m³K, the thermal conductivity is $\lambda_i = 0.21$ W/Km and the emissivity is $\varepsilon = 0.95$. The examined cable is loaded with the current 70 A. 25 °C is the environmental temperature T_e , which is as well the temperature of the whole cable at $t = 0$ s (T_0). The beginning (T_1) and the end (T_2) of the cable have the temperature 50 °C.

As reference solution T_{pdepe} , the numerical solution of the partial differential equation (1) of the problem is calculated using the function pdepe of MATLAB (MathWorks, 2020). Generally, partial differential equations of the form (18) with initial conditions $u(x, 0)$ and boundary conditions (19) are solved by this function. As in the concrete problem, the cable surface temperature T_s is necessary for the calculation of the parameters of the equivalent circuit, the formulation (20) is implemented. The nonlinear material parameters are directly considered here, so further iterations are not necessary.

$$\begin{aligned} c(x, t, u, \partial u / \partial x) \partial u / \partial t &= s(x, t, u, \partial u / \partial x) \\ &+ x^{-m} \partial (x^m f(x, t, u, \partial u / \partial x)) / \partial x \end{aligned} \quad (18)$$

$$p(x, t, u) + q(x, t) f(x, t, u, \partial u / \partial x) = 0 \quad (19)$$

$$u = (T \quad T_s)^T, x = z, \quad (20)$$

$$\begin{aligned} A \partial T / \partial t &= \partial^2 T / \partial z^2 - B(T_s)T + C(T, T_s), \\ 0 &= 0 + T - T_s - R'_\lambda(T - T_e)G'(T_s). \end{aligned}$$

4.1 Convergence Behavior

In Figure 4, the convergence of the sums appearing in the above presented solutions is evaluated. The deviation from the numerically calculated temperature $\Delta T = |T - T_{pdepe}|$ is shown here. A cable of the very short length $L = 0.1$ m is examined as later on in this paper, it is shown, that especially for short cables, the new solutions drastically improve the accuracy of the predicted temperatures. For comparison, the results calculated via the old approximation solution are given. As can be seen, those lead to much higher deviations than the new solutions. The series solution derived via Green's functions in the time domain and the series solution for $T_1 = T_2$ from the Laplace

domain converge very fast. Unlike, the series solution considering the boundary conditions $T_1 \neq T_2$ shows a bad convergence behavior. In this solution, instead of the position $z = 0$ m, the slightly higher value $z = 1$ mm is inserted in the calculation because of the unsteady behavior of the solution at this position. Because of the bad convergence, this solution is not applicable for the solution of real problems and will not be further evaluated in the following.

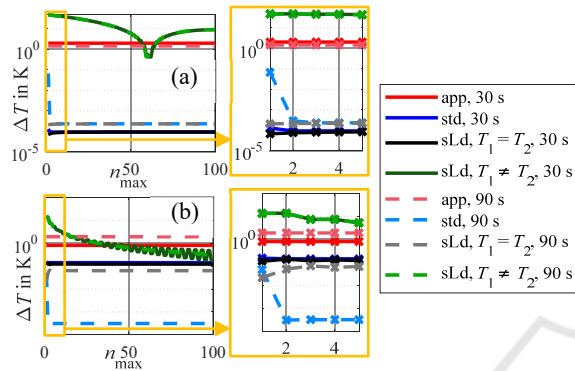


Figure 4: Deviation between analytically (approximation (app), series time domain (std), series Laplace domain (sLd)) and numerically calculated temperatures depending on the number of addends at (a) the beginning and (b) the middle of the cable.

4.2 Validation with Numerical Solution

Now, a cable with the length $L = 1$ m is evaluated. In Figure 5(a), the cable temperature calculated with the numerical reference solution is shown depending on the time t and the spatial coordinate z . In Figure 5(b), for three cases, the results calculated via the numerical reference solution and via the three analytical solutions are compared: The transient temperature development is evaluated at $z = 0.5$ m (middle of the cable). For the times $t = 200$ s (transient area) and $t = 600$ s (stationary), the axial temperature development along the cable is evaluated. Here, for the new solution “series (time domain)” based on the Green’s functions in the time domain, only one addend from the sum is taken into account, for the solution based on the Green’s functions in the Laplace domain (“series (Laplace domain)”), 10 addends are used. As shown in Figure 5(c) for the position $z = 0.5$ m, convergence is not reached for this number of terms. Nevertheless, the usage of so few terms is evaluated here as in practical applications, also only a low number of terms can be considered due to restricted calculation power. All of the presented solutions show a similar development. So, for this case, all three solutions can be used.

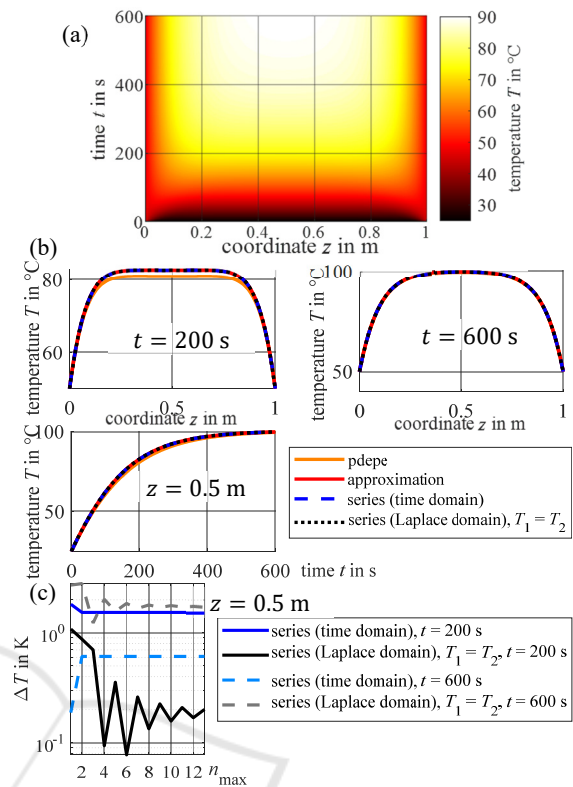


Figure 5: Results for the cable length 1 m. (a) Numerical reference solution. (b) Results for fixed position respectively time. (c) Convergence behavior example.

For a very short cable, the approximation used in the solution from the Laplace domain (Henke and Frei, 2020) is not valid anymore. That is why for short cables, huge deviations between the old solution and the reference solution are expected. To evaluate the performance of the newly derived solutions, the calculation is repeated for a cable with the length $L = 0.1$ m. In Figure 6, the results are presented. Because of the short cable length, the conductor temperature in the middle of the cable is much lower than before as the cable ends cool the cable in this example (see Figure 6(a)). In Figure 6(b), it is shown, that the solution resulting from the Laplace domain without Green’s functions is not able to model the temperature development correctly, but, as expected, massive deviations appear. The set boundary conditions at the cable ends are not fulfilled anymore. If just one addend of the sum resulting from the Green’s function solution in the time domain (solution “series (time domain)”) is added, the result matches to the numerical reference solution much better. The solution based on Green’s functions in the Laplace domain (“series (Laplace domain)”) also predicts the correct temperatures quite well. As can be seen for the

time $t = 30$ s, in the transient case, both series solutions show noticeable deviations to the numerical reference solution, but those are much lower than 1 K. Furthermore, the set boundary conditions are fulfilled by both solutions. So, all in all, for this very short cable, the usage of the new series solutions massively improves the accuracy of the predicted temperatures.

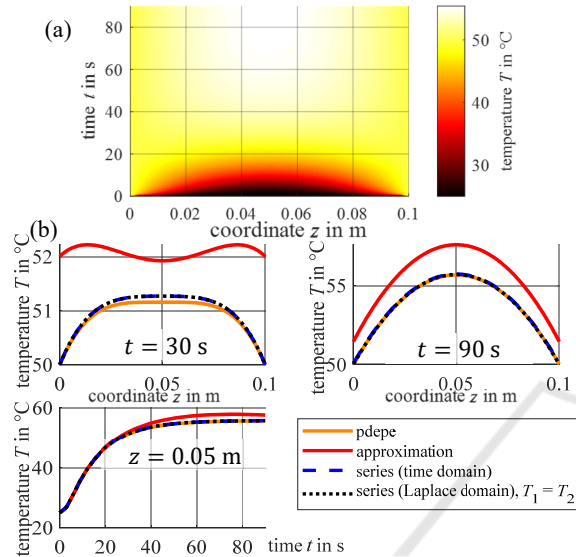


Figure 6: Results for the cable length 0.1 m. (a) Numerical reference solution. (b) Results for fixed position respectively time.

4.3 Influence of the Cable Length

As shown in Figure 6, for short cables, the approximation causes deviations from the numerical solution. For the stationary case, even the set boundary conditions (cable end temperatures) are not calculated correctly. In Figure 7, this effect is studied. The dependency of the deviation between the different analytical solutions and the numerical reference solution from the cable length is presented for the time $t = 1000$ s at the beginning of the cable ($z = 0$ m) and in the middle of the cable ($z = 0.5 L$). As can be seen for the cable beginning, for short cables, the deviation of the Laplace approximation grows exponentially. Using the new solutions based on the usage of Green's functions in the time domain by simply adding one more term improves the results, but for cable lengths below 0.4 m, rising deviations appear as well. Using more terms (shown for 5 addends here) ensures a stable behavior in the complete evaluated area down to 0.1 m. The same behaviour is also observed using the series solution from the Laplace domain for identical cable end temperatures $T_1 = T_2$ (10 addends). In the middle of

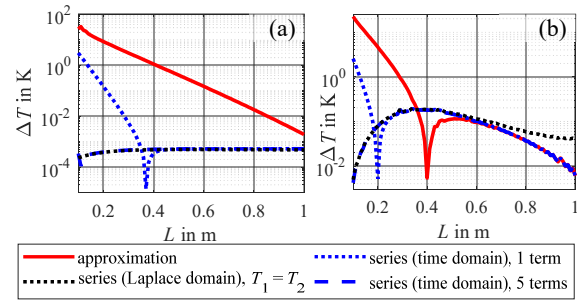


Figure 7: Deviation between the analytically and numerically calculated temperatures depending on the cable length at (a) the beginning and (b) the middle of the cable.

the cable, also, for short cables, using the new solutions improves the accuracy of the solution. For longer cables, the series solution from the Laplace domain shows a worse accuracy. Here, more terms need to be taken into account to improve this. So especially for short cables, the new solutions can improve the results. By changing the number of addends that is used in the solutions, the accuracy of the solutions can directly be adapted.

Also, the cable cross-section area influences the deviations. A critical cable length L_{crit} is introduced, under which the Laplace approximation cannot be used any longer. This critical cable length is defined as the cable length, at which the deviation for the stationary temperature in the middle of the cable exceeds 3 K. The critical cable length is calculated for different cables that are characterized by their conductor radius r_c . For each cable length, the current through the cable is chosen so that the stationary temperature in the middle of the cable is (100 ± 0.2) °C. Using the bisection method, this current and the corresponding critical cable lengths are found. For the cable length, an uncertainty of 1 mm is allowed as stop criterion. The results are shown in Figure 8. A linear correspondence between the critical cable length and the conductor radius is observed: The smaller the cable conductor radius, the shorter the critical cable length is. So especially for short cables with a high cross section, the approximation from (Henke and Frei, 2020) cannot be used as its accuracy is very bad there. Then, the new solutions can replace this method as analytical calculation approaches.

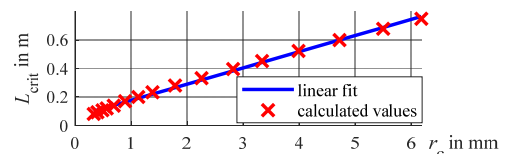


Figure 8: Critical cable length depending on conductor radius.

4.4 Complexity Considerations

The numerical complexity has a major impact on the runtime and practical applicability. Here, for the analysis of the complexity of the different solutions, only the appearance of functions as the exponential function, the error function or the sine in the final calculation formula are compared. The square root and the calculation of the cable parameters are not considered here. In the solution from the time domain, the approximation from the Laplace domain without Green's functions (11 function evaluations) appears again. Each additional term from the sum goes with 20 function evaluations. Compared to that, the evaluation of a single term from the solution from the Laplace domain Green's functions takes much less effort (2 function evaluations). This rough estimation of the complexities of the different approaches also motivates the above used number of terms: Taking one additional term into account for the series solution in the time domain results in a total number of 31 function evaluations, whereas 20 evaluations are necessary for the series solution in the Laplace domain. So, although a higher number of addends is taken into account, the series solution in the Laplace domain causes less calculation effort.

5 APPLICATION EXAMPLE

The standard ISO 6722 defines critical insulation temperatures based on the insulation aging due to thermal stress. For PVC, the continuous operation temperature (3000 hours) is $T_{3000h} = 105\text{ }^\circ\text{C}$. The corresponding short-term temperature (240 hours) is $T_{240h} = 130\text{ }^\circ\text{C}$ and the thermal overload temperature (6 hours) is $T_{6h} = 155\text{ }^\circ\text{C}$. So, on the one hand, higher temperatures drastically reduce the expected lifetime of the insulation material. On the other hand, this means that thermal overload can be tolerated for a short time, if necessary, but the accelerated aging has to be considered. In Figure 9, the insulation lifespan is presented depending on the insulation temperature. For temperatures higher than T_{dec} , a degradation of the insulation occurs even after short times. If the temperature becomes higher than T_{fire} , the insulation can start to burn and operation is not possible at all. Melting fuses are supposed to keep the cable temperature in the dark green area, short-time overload situations that lead to accelerated cable aging (light green area) or the need to replace the cable afterwards (yellow area) cannot be tolerated. Unlike, intelligent fuses can support controlled overload situations.

In Figure 10, a possible use-case for overload handling using simple melting fuses on the one hand and intelligent fuses on the other hand is presented. In case of a simple melting fuse, if the fuse trips, a hard interruption of functions results, which causes an undefined and potentially unsecure state of the complete system. Using an intelligent fuse, the overload is detected but the cable is not directly disconnected. First, the advanced driver assistance systems (ADAS) controller is asked whether an emergency operation is necessary. In case of a requested emergency operation the cable can be operated in the light green or even yellow area of Figure 9. This way, in many cases, a defined and safe state can be achieved by controlled measures, and afterwards it can be decided whether the cable has to be replaced. The safety and reliability of the complete system is massively improved.

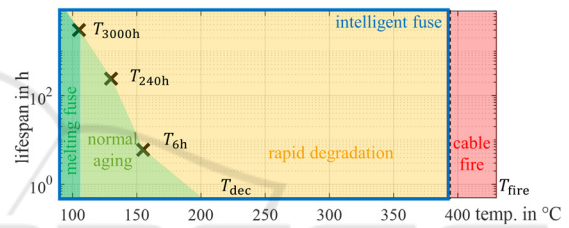


Figure 9: Lifespan of the cable insulation depending on the insulation temperature with different operating regions.

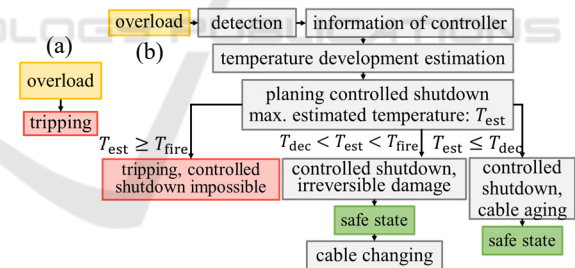


Figure 10: Overload handling with (a) melting fuses and (b) PDU in combination with intelligent fuses.

An example is shown in Figure 11: A 48 V ADAS controller has a power consumption of 2 kW. The power supply is realized via a PDU with intelligent fuses. The cable that connects the PDU and the ADAS controller has a length of 3 m and is dimensioned for a rated current of 42 A. Maximum environmental and contact temperatures of $T_e = T_1 = T_2 = 85\text{ }^\circ\text{C}$ are assumed. Then, to ensure a temperature below $T_{3000h} = 105\text{ }^\circ\text{C}$, a cable with a cross-section area of 10 mm^2 is necessary (stationary maximal cable temperature: $99.0\text{ }^\circ\text{C}$). It is assumed now that due to a failure the power consumption of

the ADAS controller rises to 4 kW at $t = 0$ s, but essential functions still work (partial failure). Then, the current through the cable rises as well: $I_{\text{error}} \approx 83$ A. Assuming an initial cable temperature of 100 °C, the corresponding cable temperature development in the middle of the cable (hottest spot) is shown in Figure 12. After 27 s, the temperature $T_{3000h} = 105$ °C is reached. A melting fuse would break the circuit here to protect the cable and automated driving applications would not be possible any longer. In contrast, in an intelligent fusing PDU, the actual cable temperature and cable aging can be considered: The short-term temperature $T_{240h} = 130$ °C is reached after about 290 s. The critical thermal overload temperature $T_{6h} = 155$ °C is not reached at all as the maximum longterm temperature is 138 °C. Therefore, an intelligent fuse does not trip, but monitors the cable aging. Automated driving is still possible, and the vehicle can be transferred into a safe state by performing a controlled shutdown.

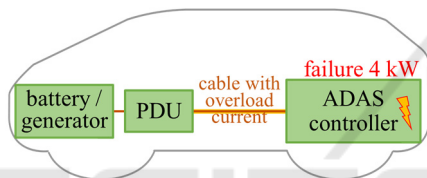


Figure 11: Simple application example for the use in intelligent vehicles.

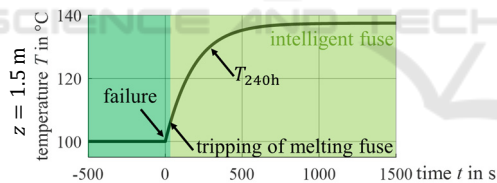


Figure 12: Cable temperature development for the application example.

6 CONCLUSIONS

In this paper, two new approaches for the analytical transient axial temperature calculation of single cables were presented. Those approaches are based on the use of Green's functions in the time domain respectively Laplace domain. The results are series representations. By choosing an appropriate number of addends, a high accuracy of the proposed methods can be obtained even for short cables. A constant cable temperature at the beginning of the calculation time, constant cable termination temperatures, a constant current through the cable and a constant ambient temperature are assumed. Regarding

applications for example for intelligent vehicles, the presented solutions can be used as fast approach for the temperature calculation in cables and therefore provide a basis for decisions in time- and safety-critical environments.

The presented example shows the potential of analytical solutions that can deal with limited resources and still model the essential thermal effects with an accuracy that allows them to be used in protective applications. In the example, a melting fuse would break the circuit due to an overcurrent and automated driving would not be possible any longer. Unlike, using a smart fuse with the presented analytical methods, the overcurrent can be tolerated and a controlled shutdown is enabled.

ACKNOWLEDGEMENTS

The work for this contribution was partly financed by the European Fund for regional development (EFRE), Ministerium für Wirtschaft, Innovation, Digitalisierung und Energie of the State of North Rhine-Westphalia as part of the AFFiAncE project.

REFERENCES

- Antonini, G., 2008. A Dyadic Green's Function Based Method for the Transient Analysis of Lossy and Dispersive Multiconductor Transmission Lines. In *IEEE Trans. Microw. Theory Techn.*, 56(4), 880-895.
- Brabetz, L., Ayeb, M., Neumeier, H., 2011. A new approach to the thermal analysis of electrical distribution systems. In *SAE Technical Paper*.
- He, J., Tang, Y., Wei, B., Li, J., Ren, L., Shi, J., Wu, K., Li, X., Xu, Y., Wang, S., 2013. Thermal Analysis of HTS Power Cable Using 3-D FEM Model. In *IEEE Trans. Appl. Supercond.*, 23(3), 5402404-5402404.
- Henke, A., Frei, S., 2020. Transient Temperature Calculation in a Single Cable Using an Analytic Approach. In *JFFHMT*, 2020(7), 58-65.
- Holyk, C., Liess, H.-D., Grondel, S., Kanbach, H., Loos, F., 2014. Simulation and measurement of the steady-state temperature in multi-core cables. In *Electric Power Systems Research*, 116, 54-66.
- Horn, M., Brabetz, L., Ayeb, M., 2018. Data-driven modeling and simulation of thermal fuses. In *IEEE Int. Conf. ESARS-ITEC*, 1-7.
- Kong, W., Luo, Y., Qin, Z., Qi, Y., Lian, X., 2019. Comprehensive Fault Diagnosis and Fault-Tolerant Protection of In-Vehicle Intelligent Electric Power Supply Network. In *IEEE Trans. Veh. Technol.*, 68(11), 10453-10464.
- MathWorks, 10.11.2020. Documentation pdepe: <https://de.mathworks.com/help/matlab/ref/pdepe.html>.

- Olsen, R., Anders, G. J., Holboell, J., Gudmundsdóttir, U. S., 2013. Modelling of dynamic transmission cable temperature considering soil-specific heat, thermal resistivity, and precipitation. In *IEEE Trans. Power Del.*, 28(3), 1909–1917.
- Önal, S., Henke, A., Frei, S., 2020. Switching Strategies for Smart Fuses Based on Thermal Models of Different Complexity. In *Int. Conf. EVER*, 1-10.
- Zhan, Q., Ruan, J., Tang, K., Tang, L., Liu, Y., Li, H., Ou, X., 2019. Real-time calculation of three core cable conductor temperature based on thermal circuit model with thermal resistance correction. In *The Journal of Engineering*, 2019(16), 2036–2041.

